

An Experimental Study on the Vibration of the Low-Speed Maglev Train Moving on the Guideway with Sag Vertical Curves

Youngang Sun^{1,2}, Wanli Li¹, Haiyan Qiang^{2*} and Daofang Chang²

¹*School of Mechanical Engineering, Tongji University, 201804, China*

²*College of Logistics Engineering, Shanghai Maritime University, 201306, China*

**Corresponding author: 1989yoga@tongji.edu.cn*

Abstract

The low-speed maglev transportation technology is becoming a new type of urban rail transit. The vibration of the train is the crucial point for comfort and performance of the new type transit. The trial operation of the low-speed maglev train shows that a strong vibration of the vehicle may occur when the vehicle moves on the rail with sag vertical curves. In order to analyze and prevent this problem, a multi-sensor low-speed maglev vehicle experimental platform is established. The vibration signals are collected, processed and analyzed by the experiment. We present that the spiral transition curve should be put into the rail to reduce the vibration. The experimental results are included to provide valuable reference for the design and construction of the low-speed maglev transportation line.

Keywords: *Maglev vehicle, vibration, sag vertical curves, multi-sensor platform, mathematic model*

1. Introduction

Owing to its commercial, environmental and technological attractions, the low-speed maglev transportation technology is becoming a new type of urban rail transit [1-4]. Compared with wheel-rail train, the low-speed maglev train has better turning and climbing capacity and saves the engineering works and cost. Compared with the urban rail transit, the low-speed maglev train has the characteristics of safety, environmental protection, comfort, rapidity, low energy consumption and low cost and especially it is suitable for in urban mass transit. The structure and its principle of the low-speed maglev train are shown in Figure 1. The basic principle of the maglev train is that utilize the electromagnetic force to overcome the earth gravity, and make the maglev train levitate on the rail. The air gap between the train and the rail is about 8mm for EMS type low-speed maglev train. The linear motor is used to push the low-speed maglev train forward.

With the actual development situation of the urban passenger rail transit, developing rail transit in large and medium sized cities is one of fundamental approaches to solve the transport difficulties. It is more necessary to develop the new type of rail transit with less investment and high efficiency (e.g., the low-speed maglev transportation). At present, many cities in China have shown great interest in the low-speed maglev transportation [5, 6]. A low-speed Maglev Test Line has been constructed successfully in Lingang new city by Shanghai municipal government, which provides the experiment environment to this study. When we drove the train moves on a rail with sag vertical curves, the low-speed maglev train showed a strong vibration of the vehicle, which should be tested and analyzed in depth. Unfortunately, there is little research on the vibration of the low-speed maglev train moving on a rail with sag vertical curves. The kinematic requirements of bogie for the maglev train to realize the mechanical decoupling based on the D-H transform is proposed by Zhang Kun [7] and Zhang Geng [8]. But they didn't figure out the bogie frame's dynamics or vibration analysis. Sun [9]

introduced the vibration information of the rail into the designed controller and proposed a feedback controller to eliminate the coupling vibration effectively. Zhou [10] established the multi-DOF dynamic model of low-speed maglev train bogie and through simulation to verify the stability of the maglev train bogie. But, they did not considering the whole train and sag vertical curves.

In this work, we built a multi-sensor low-speed maglev vehicle experimental platform to test the vibration when the train moves on a rail with sag vertical curves. The vibration of the maglev train on the upslope and the train into the sag vertical curves were tested respectively. The vibration signals are collected, processed and analyzed by the experimental platform. The experimental results are presented to provide valuable reference for the design and construction of the low-speed maglev transportation line.

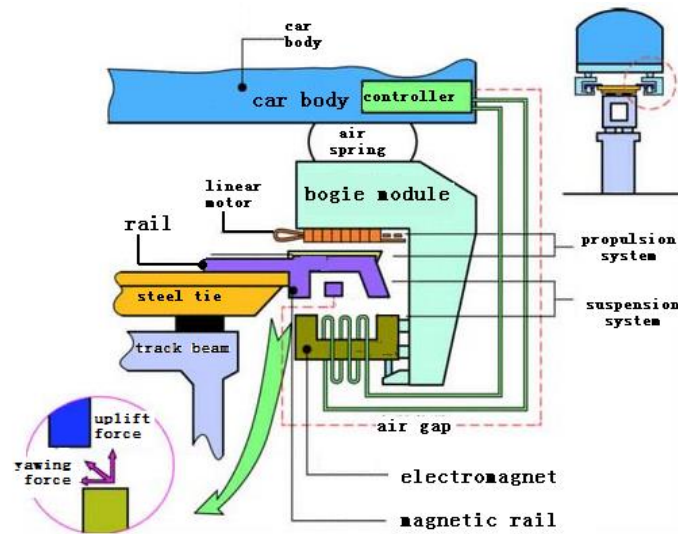


Figure 1. Configuration of the Low-Speed Maglev Train

2. Mathematic Model of the Vibration for Maglev Train

The vibration model for maglev train can be simplified to spring-damping system as shown in Figure 2.

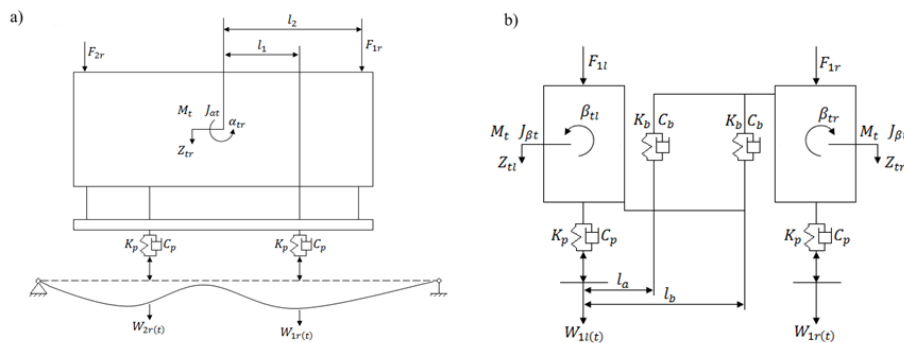


Figure 2. Simplified Vibration Model

The left of the Figure 2 shows the force of the front side of the train. Right of Figure 2 shows the force of the right side of the bogie frame. So we can get the overall force of the train. Assuming the car body as a rigid body, it can be simplified as a vibration system composed of two rigid bodies, which are connected with each

other by the elastic damping element (K_b , C_b). Each rigid body has three degrees of freedom, which are vertical, pitching and rolling. The vertical levitation force of the electromagnet in single EMS module is equivalent to the spring damper suspension model (K_p , C_p). According to Figure 2, we can get the whole vibration model in the directions of vertical, pitching and rolling [11, 13].

Vertical:

$$\begin{cases} m_l \ddot{z}_l = \sum_{i=1}^2 F_{li} - \sum_{i=1}^2 K_p (2z_l - W_{li}) + m_l g - \sum_{i=1}^2 C_p (2\dot{z}_l - \dot{W}_{li}) \\ m_r \ddot{z}_r = -\sum_{i=1}^2 C_p (2\dot{z}_r - \dot{W}_{ri}) - \sum_{i=1}^2 K_p (2z_r - W_{ri}) + \sum_{i=1}^2 F_{ri} + m_r g \end{cases} \quad (1)$$

Pitching:

$$\begin{cases} J_{\alpha l} \ddot{\alpha}_l = -C_p [2l_1^2 \dot{\alpha}_l + l_1 (\dot{W}_{l1} - \dot{W}_{l2})] + (F_{l1} - F_{l2})l_2 - K_p [2l_1^2 \alpha_l + l_1 (W_{l1} - W_{l2})] \\ J_{\alpha r} \ddot{\alpha}_r = (F_{r1} - F_{r2})l_2 - K_p [2l_1^2 \alpha_r + l_1 (W_{r1} - W_{r2})] - C_p [2l_1^2 \dot{\alpha}_r + l_1 (\dot{W}_{r1} - \dot{W}_{r2})] \end{cases} \quad (2)$$

Rolling:

$$\begin{cases} J_{\beta l} \ddot{\beta}_l = 2l_a l_b \beta_l + (l_a + l_b)(z_l - z_r)] + 2K_p \beta_l - K_b [(l_a^2 + l_b^2) \beta_l - 2C_p \dot{\beta}_l \\ \quad - C_b [(l_a^2 + l_b^2) \dot{\beta}_l + 2l_a l_b \dot{\beta}_l + (l_a + l_b)(\dot{z}_l - \dot{z}_r)] \\ J_{\beta r} \ddot{\beta}_r = 2l_a l_b \beta_r - (l_a + l_b)(z_l - z_r)] + 2K_p \beta_r - 2C_p \dot{\beta}_r - K_b [(l_a^2 + l_b^2) \beta_r \\ \quad - C_b [(l_a^2 + l_b^2) \dot{\beta}_r + 2l_a l_b \dot{\beta}_r - (l_a + l_b)(\dot{z}_l - \dot{z}_r)] \end{cases} \quad (3)$$

where, F_{l1} , F_{r1} , F_{l2} and F_{r2} denote vertical loads from air springs of left front, right front, left rear and right rear to the train body respectively; W_{l1} , W_{r1} , W_{l2} and W_{r2} denote the electromagnetic forces of left front, right front, left rear and right rear the corresponding track irregularity; z_{l1} , z_{tr} , α_{l1} , α_{tr} , β_{l1} and β_{tr} denote heaving displacement, pitching angle and rolling angle of left and right side of train body.

We can obtain the fact from the mathematic model of the vibration that the model can be used for simple vibration analysis. But the vibration of the vehicle with the vehicle moving on a guideway with sag vertical curves is rather complex, which can be related to altitude valve, sliding bearing, air spring, currents, suspension controller and so many components. The mathematic model cannot be used to study the complex problem. So, a multi-sensor low-speed maglev vehicle experimental platform should be established.

3. Multi-Sensors Layout on the Maglev Train

The test low-speed maglev vehicle is shown in figure 3. In order to facilitate the analysis, the sensors must be numbered. Besides transverse sliding bearing, the measure points of suspension, guide, vibration acceleration, displacement of air spring and current are numbered as Figure 4. The measure points' numbers of air spring stress are shown in Figure 5.

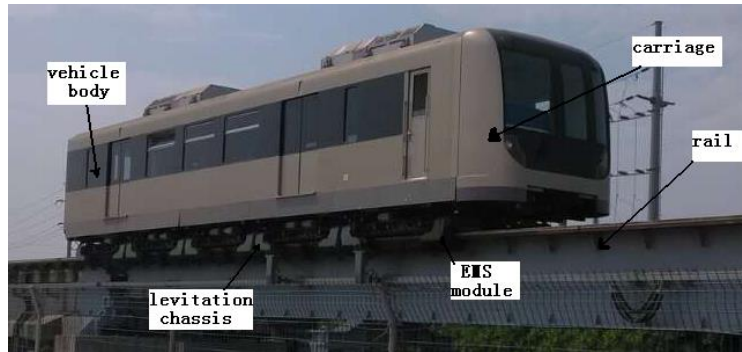


Figure 3. Structure of the Maglev Train

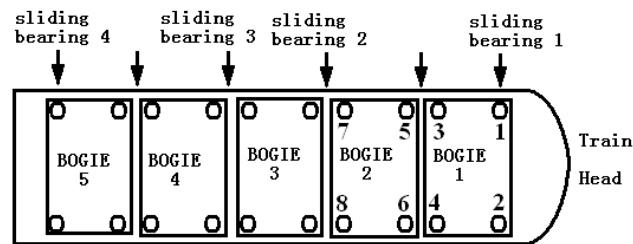


Figure 4. Serial Numbers of Measure Points

The position and speed detection signals are introduced from position and speed detection device to data acquisition and analysis system. The acceleration sensors are placed in suitable positions of the surface of the electromagnets in bogie 1 and 2. The output cables of the acceleration sensors are also connected to the data acquisition and analysis system. There are four acceleration sensors placed in a single bogie. Totally eight piezoelectric crystal acceleration sensors are utilized. The installation locations in the bogies are shown in the Figure 6. Also, the vertical air gap sensors and lateral air gap sensors are put in suitable positions of the surface of the electromagnets in bogie 1 and 2. There are four vertical air gap sensors and four lateral air gap sensors placed in a single bogie. The air gap sensors and guide gap sensors are eddy-current sensors. All the installation locations of these sensors in the bogies are shown in the Figure 6. Since the test precision of the method of surface bond strain gauge for the air springs cannot meet the test requirement, we choose air stress sensors to measure the stress of the air springs. The layout of the measure points are shown in Figure 5.

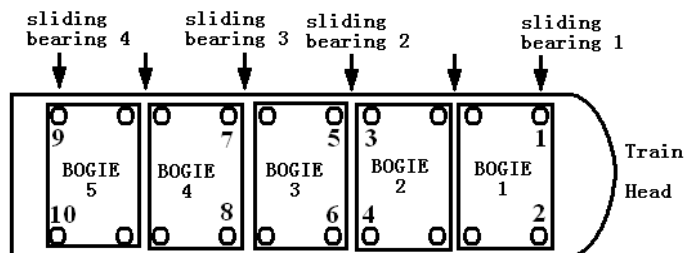
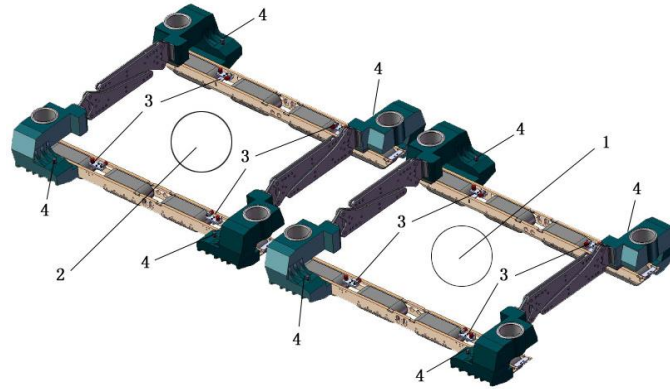


Figure 5. Measure Points' Numbers of Air Spring Stress



1-bogie 1; 2-bogie 2; 3-vertical and lateral air gap sensors; 4-acceleration sensors

Figure 6. Installation Diagram For The Acceleration, Vertical And Lateral Air Gap Sensors

As shown in Figure 4, the displacement sensors are installed on the air springs of bogie 1 and bogie 2. The displacement sensors should be fixed in the bogies. The maximum displacement of the air spring is about 30mm and frequency below 5Hz. So, we choose inductive or strain type displacement sensors. The layout of the displacement sensors are shown in Figure 7.

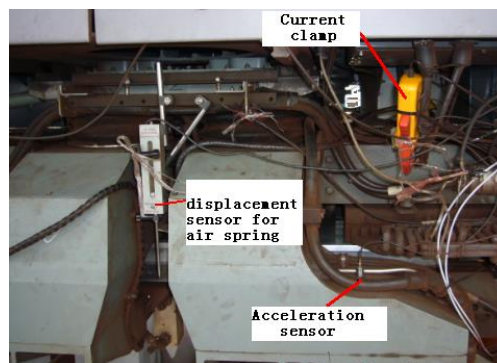


Figure 7. The Installation Position of Sensors

In order to measure the displacement of the lateral bearing, the displacement sensors are placed in the lateral bearings. Considering the displacement of the lateral bearing could be 450mm, sliding resistance type sensors with 500mm measuring range are utilized. The installation positions of the sensors are shown in Figure 8. The current measure of the electromagnet coil adopted the current clamp as shown in Figure 7.

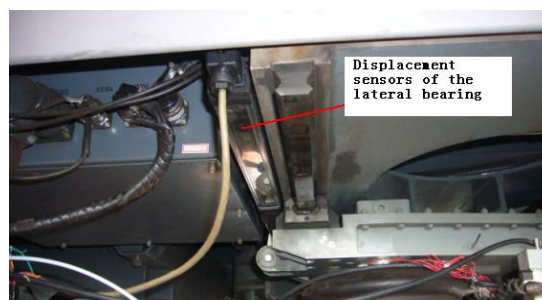


Figure 8. Installation Position of Sensors for the Lateral Bearing

4. The Vibration of the Maglev Train into the Sag Vertical Curves

In order to measure the vibration signals of the train, the test train was driven into the sag vertical curve. When the vibration occurred, we stopped the train and collect the vibration signals.

Firstly, 4 altitude valves were used by the test train. The displacement and velocity of the train are shown in Figure 9 and Figure 10.

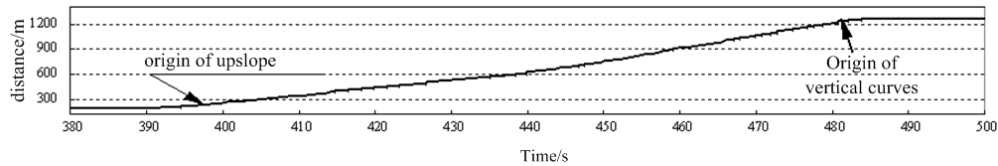


Figure 9. Position of the Maglev Train

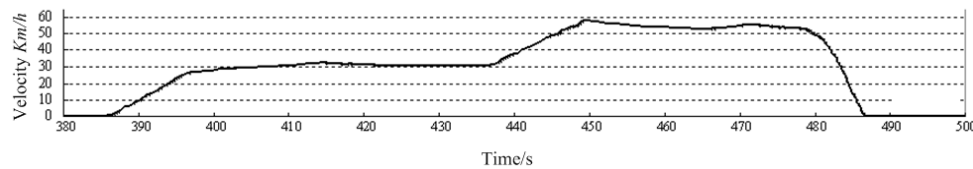


Figure 10. Velocity of the Maglev Train

The Stress of air springs is shown in Figure 11. We can obtain from the Figure 11 that the Stress of air spring 1 and air spring 2 had a large variation, but the others changed slightly when the time was 490 second.

The vibration acceleration of the bogie is shown in Figure 12. From the graph it is evident that when the train was driven into the sag vertical curve, the train began to vibrate and there was big vibration acceleration of the bogie. The maximum vibration acceleration was more than 100g. However, the normal vibration acceleration of the bogie should be about 1g.

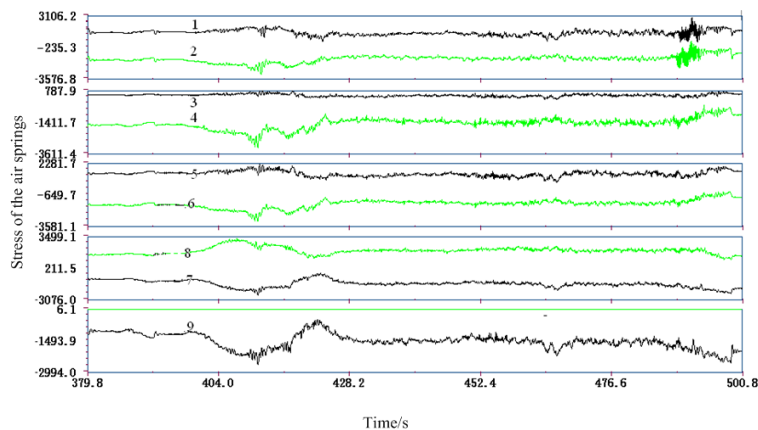


Figure 11. Stress of Air Springs with the Train Up the Upslope

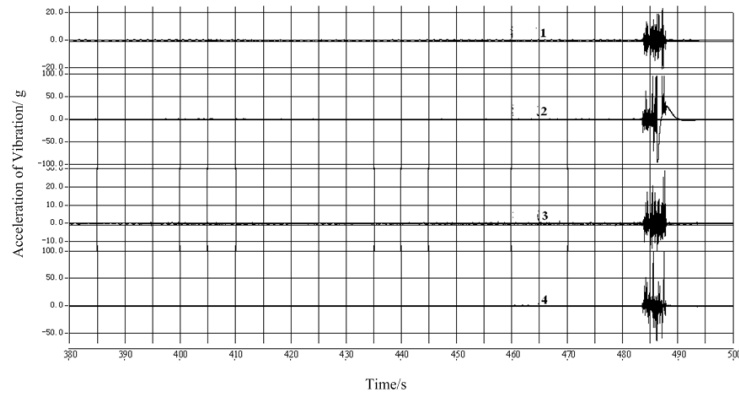


Figure 12. Acceleration of the Bogie with the Train Up the Upslope

Just like the vibration acceleration of the bogie, the displacement of air springs had high-frequency variation, when the train was driven into the sag vertical curve. The values of the displacement were more than the other place, which can be seen in Figure 13.

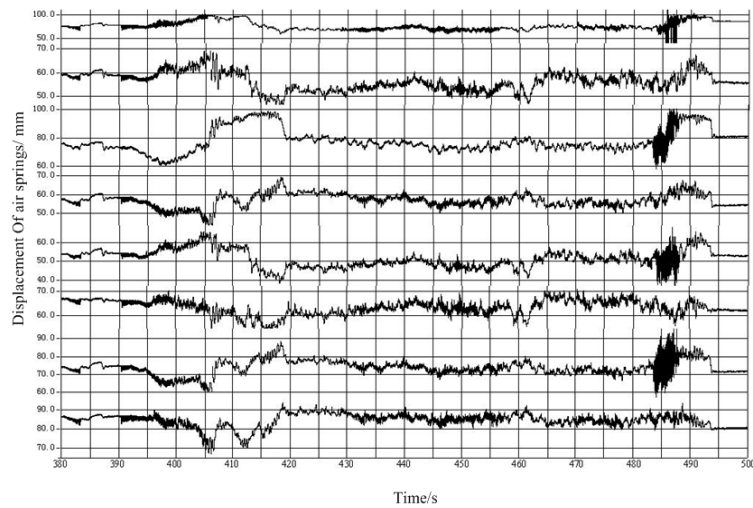


Figure 13. Displacement of Air Springs of the Train

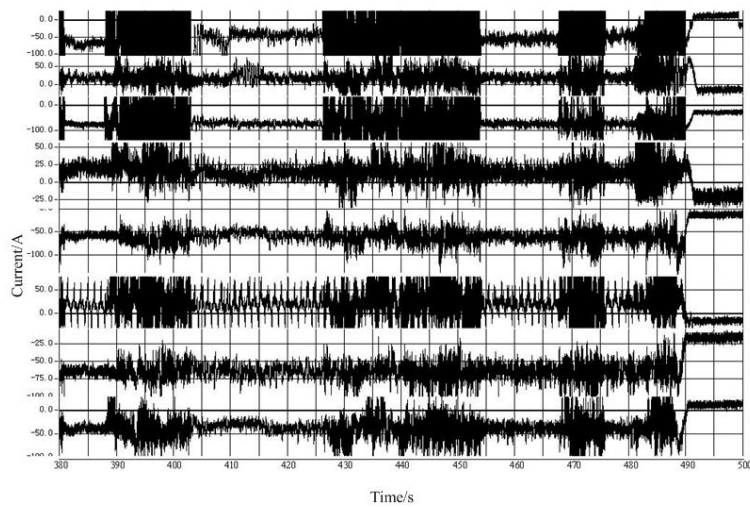


Figure 14. Current of Electromagnet with Train Up the Upslope

When the train was in a state of traction, the traction motor current had a great influence on the current clamp, which meant test signals have large noise shown in Figure 14. We can find from the Figure 14 that the maximum current was more than 100A. In order to study the influence of the number of the altitude valve, we collected the vibration signals of the train with 3 altitude valves and the train with 4 altitude valves, respectively. The test results of measure point 2 were given in Figure 15 and Figure 16 to know the change conditions of all kinds of vibration signals.

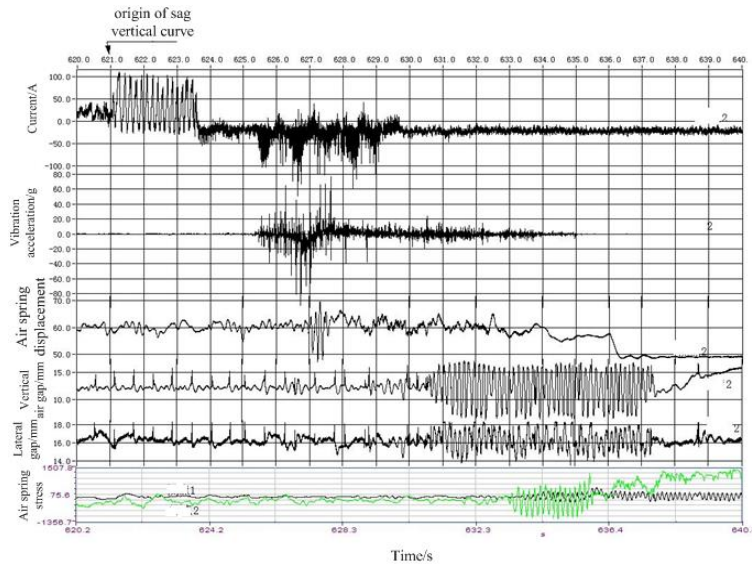


Figure 15. Vibration of the Measure Point 2 with Three Altitude Valves

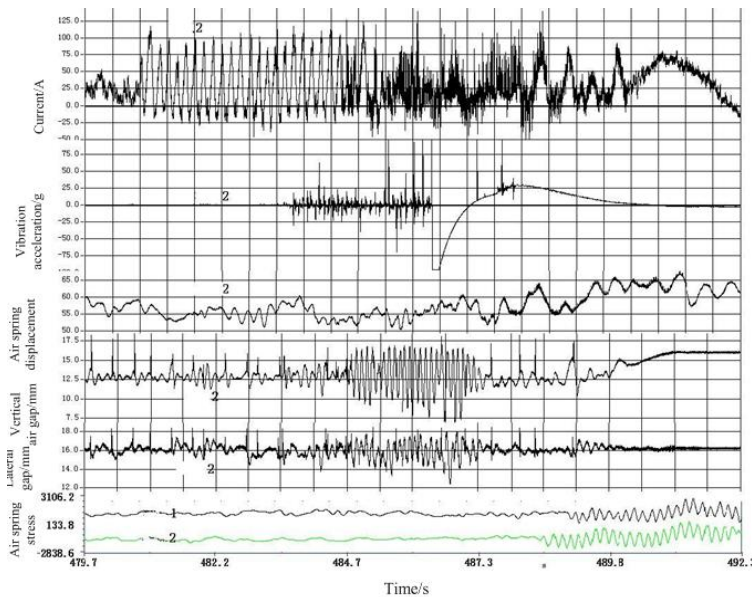


Figure 16. Vibration of the Measure Point 2 with Four Altitude Valves

The test train with three altitude valves began to vibrate when the train into the sag vertical curve. It can be seen from the Figure 15 that once the train began to vibrate, the bogie, stress of air springs, displacement of air springs, current, vertical and lateral air gap all had obvious fluctuation.

The vibration of the train with four altitude valves was very similar to the train with three altitude valves, which was shown in Figure 16. The air gap had little change with

the maximum air gap less than 12mm. The variation of the stress of air springs was less than 1000N. In terms of distribution, the positive and negative change value of the air springs stress was basically equal.

6. Conclusion

In this paper, we built a multi-sensor low-speed maglev vehicle experimental platform to test the vibration signals when the train moves on a rail with sag vertical curves. The different vibration types of the maglev train into the sag vertical curves were tested respectively. Contrast the difference between the train with three altitude valves and four altitude valves. The vibration signals are collected, processed and analyzed by the experimental platform. The spiral transition curve should be put into the rail to reduce the vibration. The experimental results are presented to provide valuable reference for the design and construction of the low-speed maglev transportation line. Furthermore, future efforts will be directed at aspects of the elimination of vibration.

Acknowledgments

This research is supported by Key Projects in the National Science & Technology Pillar Program of China. (2013BAG19B00-01), Key Projects in the National Science & Technology Pillar Program during the Twelfth Five-year Plan Period (2011BAJ02B00).

References

- [1] R. D. Thornton, "Efficient and Affordable Maglev Opportunities in the United States", PROCEEDINGS OF THE IEEE, vol.97, no. 11, (2009), pp. 1901-1921.
- [2] H.W. Lee, K.C. Kim and J. Lee, "Review of Maglev Train Technologies", IEEE TRANSACTIONS ON MAGNETICS, vol. 42, no. 7, (2006), pp.1917-1925.
- [3] S.K. Liu, B. An, and Z. J. Guo, "Characteristic research of electromagnetic force for mixing suspension electromagnet used in low-speed maglev train", IET ELECTRIC POWER APPLICATIONS, vol. 9, no. 3, (2015), pp. 223-228.
- [4] K. J. Kim, H. S. Han and S. J. Yang, "Air gap control simulation of maglev vehicles with feedback control system", International Journal of Control and Automation, vol. 6, no. 6, (2013), pp. 401-412.
- [5] P. Z. Zhang, "Research on the Technology for the Self- innovation of Low/Medium- speed Maglev Traffic Engineering", Journal Of Railway Engineering Society, no.10, (2009), pp.90-94.
- [6] Q. B. Peng, "Technology and Engineering Application of Mid-low Speed Maglev Transportation System", Electric Drive for Locomotives, no.3, (2014), pp. 6-9.
- [7] G. Zhang, J. Li and J. H. Li, "Kinematics Study on Anti-roll Boom of Low-speed Maglev train", Journal of the China Railway Society, vol. 34, no. 4, (2012), pp. 28-33.
- [8] K. Zhang, J. Li and W. S. Chang, "Structure Decoupling Analysis of Maglev Train Bogies", Electric Drive for Locomotives, no.1, (2005), pp. 22-29.
- [9] Y.G. Sun, H.Y. Qiang, G.B.Lin, J.D. Ren and W.L. Li. "Dynamic Modeling and control of nonlinear electromagnetic suspension systems", Chemical Engineering Transactions, vol.46, (2015), pp. 1039-1044.
- [10] Y. Zhou, F. Liu, X. K. Li and Z. H. Chi, "Vertical Dynamics Analysis of Levitation Chassis on Middle and Low Speed Maglev Vehicle", Machine Design and Research, vol. 28, no. 5, (2012), pp. 4-7.
- [11] Z. Y. Liu, W. X. Deng and P. Gong, "Dynamics of the Bogie of Maglev Train with Distributed Magnetic Forces", Shock and Vibration, vol.2015, Article ID: 896410, (2015).
- [12] Y. G. Sun, W.L. Li, D. S. Dong, X. Mei and H. Y. Qiang, "Dynamics Analysis and Active Control of a Floating Crane", Tehnicki Vjesnik-Technical Gazette, vol. 22, no. 6, (2015), pp. 1383-1391.
- [13] Z. Y. Liu, W. X. Deng and P. Gong, "Dynamics-control Modeling and Analysis for Bogie of Low-speed Maglev Train", Journal of the China Railway Society, vol. 36, no. 9, (2014), pp. 39-43.

Authors



Sun Yougang. He received his M.Sc. in Mechatronics Engineering (2013) from Shanghai Maritime University. Now he is a PhD Candidate in Tongji University. His current research interests include aspects of Dynamic systems and Non-linear control.



Wanli Li. She received her Ph.D. degree in mechanical engineering from Tongji University, China. She has been a professor and Doctoral tutor in Tongji University, China. Her current research interests include construction machinery, maglev train, intelligent control.



Haiyan Qiang. She received her M.Sc. in Mechatronic Engineering (2013) from Shanghai Maritime University. Now she is a laboratory technician of mechanical engineering at Logistics Engineering Department, Shanghai Maritime University. Her current research interests include mathematical modeling, multi-body dynamics and modern design theories and methods.



Daofang Chang. He received his Ph.D. degree in mechanical engineering from Shanghai Jiaotong University, China, in 2012. Since 2014, he has been a professor in Shanghai Maritime University. His current research interests include intelligent decision and man-machine interaction.